Experimental Self-Testing of a Single Quantum System

Xiao-Min Hu,[1,2,*] Yi Xie,[3,4,*] Atul Singh Arora,[5,*] Ming-Zhong Ai,[1,2,*] Kishor Bharti,[6,*] Jie Zhang,[3,4] Wei Wu,[3,4] Ping-Xing Chen,[3,4,†] Jin-Ming Cui,[1,2] Bi-Heng Liu,[1,2,‡] Yun-Feng Huang,[1,2,§] Chuan-Feng Li,[1,2,¶] Guang-Can Guo,[1,2] Jérémie Roland,[5] Adán Cabello,[7,8] and Leong-Chuan Kwek[6,9,10]

[1] *CAS Key Laboratory of Quantum Information, University of Science and Technology of China, Hefei, 230026, People's Republic of China*
[2] *CAS Center For Excellence in Quantum Information and Quantum Physics, University of Science and Technology of China, Hefei, 230026, People's Republic of China*
[3] *Department of Physics, College of Liberal Arts and Sciences, National University of Defense Technology, Changsha 410073, Hunan, China*
[4] *Interdisciplinary Center for Quantum Information, National University of Defense Technology, Changsha 410073, Hunan, China*
[5] *Université libre de Bruxelles, Belgium*
[6] *Centre for Quantum Technologies, National University of Singapore, Singapore*
[7] *Departamento de Física Aplicada II, Universidad de Sevilla, E-41012 Sevilla, Spain*
[8] *Instituto Carlos I de Física Teórica y Computacional, Universidad de Sevilla, E-41012 Sevilla, Spain*
[9] *MajuLab, CNRS-UNS-NUS-NTU International Joint Research Unit, Singapore UMI 3654, Singapore*
[10] *National Institute of Education, Nanyang Technological University, Singapore 637616, Singapore*

Quantum self-testing is a powerful certification scheme for quantum systems. Analogous to Bell nonlocality, quantum contextuality is also a counter-intuitive phenomenon in quantum mechanics. In this paper, we investigate how to use quantum contextuality to realize self-testing of a single quantum system in theory and experiment. We provide the robustness curve corresponding to the local self-testing protocol based on KCBS inequality by using semidefinite programming with moment matrices. Our robustness curve renders the results of *Phys. Rev. Lett. 122, 250403 (2019)* amenable to experimental scenarios. Using a single trapped $^{40}Ca^{+}$ ion, we provide the first experimental demonstration of a local self-testing protocol. In the experiment, we close the detection efficiency loophole and use a random number generator to select the basis. The experiment realizes the original intention of self-testing and reduces our dependence on various assumptions. Our results have an important promotion for the certification of local quantum systems under minimal assumptions.

Introduction.—Understanding the internal workings of quantum devices becomes challenging and crucial with the increase in their corresponding dimensionality. The task of quantum device certification is inherently demanding due to the exponential scaling of Hilbert space as system size increases. In a faithfully minimalistic scenario, developing confidence in the inner functioning of quantum devices mandates certification schemes that require minimal assumptions regarding their functioning. One of the most potent methodologies to render guarantees regarding the internal functioning of quantum devices solely based on experimental statistics, under reasonable assumptions, is self-testing. The first self-testing protocol for a pair of non-communicating entangled quantum devices was devised in the milestone paper by Mayers and Yao in 2004, which relied on Bell nonlocality [1]. Since then, self-testing via Bell nonlocality has been exhibited for GHZ states, all pure bipartite entangled states, and all multipartite entangled states that admit a Schmidt decomposition. The idea of self-testing has been further extended to the prepare-and-measure scenario, contextuality and quantum steering. For a comprehensive review of self-testing, see reference [2].

Self-testing based on Bell nonlocality is a powerful method which allows us to acquire insights concerning the inner workings of a duo of space-like separated entangled devices. And it has been verified in the experiments [3–5]. However, for single untrusted quantum devices, self-testing based on Bell-nonlocality forfeits its relevance and one requires local self-testing schemes for such cases. Since computation typically happens locally, a quantum computer is a canonical example of a single quantum device. This necessitates the development of self-testing protocols for single untrusted quantum devices. The first local self-testing scheme was presented in reference [6] where the scheme relied on violation of non-contextuality inequalities via qutrits. Non-contextuality inequalities are linear inequalities, similar to Bell inequality, the violation of which can be used to witness non-classicality. The advantage of non-contextuality inequalities over Bell inequality is that it can be implemented for a single device and thus bypasses the non-communication assumption. In a subsequent work [7], the aforementioned scheme was generalized to arbitrarily high dimension. Using complexity-theoretic ideas, self-testing scheme for a single quantum device was shown in reference [8]. For a self-testing protocol to be of ex-

* These five authors contributed equally to this work.
† pxchen@nudt.edu.cn
‡ bhliu@ustc.edu.cn
§ hyf@ustc.edu.cn
¶ cfli@ustc.edu.cn

perimental relevance, the scheme must be robust against experimental noise. Though the self-testing scheme in [6] is robust, the robustness was proven up to multiplicative constants and hence is not directly implementable.

In this Letter, we attempt to address the limitations of reference [6] by providing the robustness curve. We utilize semidefinite programming with moment matrices to obtain the aforementioned curve. This is the first-ever robustness curve for a non-contextuality inequality for a single quantum system. Furthermore, using single trapped $^{40}Ca^{+}$ ion, we provide an experimental demonstration of the local self-testing scheme. In the experiment, we close the detection efficiency loophole and use random number generator to select the base randomly. In order to reduce the dependence of our self testing on the assumptions, we discuss the compatibility loophole and sharp measurement in experiment in detail. In the experiment, it is observed that the lower bound of the total identity of the measurements and state can be self-tested self testing by violating the KCBS inequality.

Theoretical framework.—

KCBS Inequality and Sequential Measurement.—Give the pure quantum state $\rho = |v_0\rangle\langle v_0|$ and a set of chain orthogonal vectors $|\nu_i\rangle$ as below:

$$
\begin{aligned}
&|v_0\rangle = (1,0,0)^{\mathrm{T}},\\
&|v_i\rangle = (\cos(\theta), \sin(\theta)\sin(\frac{i\pi(n-1)}{n}), \sin(\theta)\cos(\frac{i\pi(n-1)}{n}))^{\mathrm{T}},
\end{aligned}
\tag{1}
$$

in which θ satisfies $\cos^2(\theta) = \cos(\pi/n)/(1+\cos(\pi/n))$ and $1 \le i \le n$, the observables in the KCBS_n inequality could take the form of $A_i = I - 2V_i$ ($V_i = |v_i\rangle\langle v_i|$). The adjacent vectors are orthogonal ($\langle v_i | v_{i+1}\rangle = 0$), that is, corresponding A_i and A_{i+1} are compatible observables. A generalized version of the KCBS_n (n is odd) inequality for a qutrit system takes the form:

$$
\begin{aligned}
\langle \chi_5 \rangle &= \langle A_1 A_2 \rangle + \langle A_2 A_3 \rangle + \langle A_3 A_4 \rangle \\
&\quad + \langle A_4 A_5 \rangle + \langle A_5 A_1 \rangle \le -3, \\
\langle \chi_n \rangle &= \sum_{i=1}^{n-1} \langle A_i A_{i+1} \rangle + \langle A_n A_1 \rangle \le -(n-2),
\end{aligned}
\tag{2}
$$

where $\langle \cdot \rangle$ denotes the average of measurement outcomes. This inequality can be derived through an exhaustive check of all possible assignments of values ± 1 to the n variables. In quantum mechanics, one finds $\langle \chi_n \rangle = n(1-3\cos(\pi/n))/(1+\cos(\pi/n))$ are identified with the qutrit observables when $A_i = I - 2|v_i\rangle\langle v_i|$.

For the value of $\langle A_i \rangle$, the exact unitary operation U_i is performed to rotate the measurement axis from $|v_i\rangle$ to $|0\rangle$ by operation shown as a single measurement box M_i in Fig. 1. Then we can acquire $\langle A_i \rangle$ via measuring the probability in state $|0\rangle$. The correlation terms $\langle A_i A_j \rangle$ are sequentially measured as shown in Fig. 1, composed

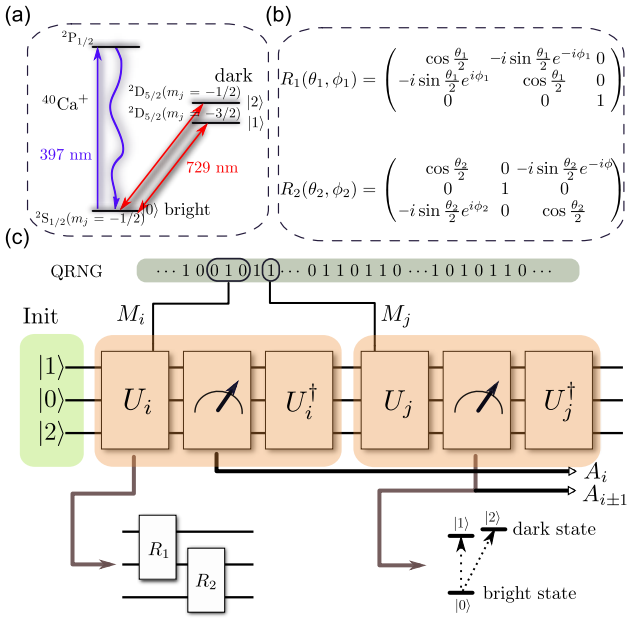

Figure 1. The $^{40}Ca^{+}$ ion system and the measurement scheme. (a) The energy level diagram of $^{40}Ca^{+}$ ion. (b) The matrix representations of $R_1(\theta_1,\phi_1), R_2(\theta_2,\phi_2)$ rotations. (c) The sequence measurement used in our experiment to measure $\langle A_i A_j \rangle$. The ion is prepared in state $|0\rangle$ initially and then measured according to block A_i , A_j orderly. The measurement of observables are chosen randomly in our experiment using a quantum random number generator (QRNG). Single observable $\langle A_i \rangle$ is measured through only block A_i. Every block includes unitary evolution, measurement and corresponding inverse unitary operation, in which the unitary operation is consist of R_1 and R_2 coherent rotation. The result is acquired via judging the number of photons collected from PMT within $220\mu s$. The statistical probability is calculated through the same measurement 10000 times. We use calcium ions, in which there are two dark states and one bright state corresponding to the eigenstate $a = 1$ and $a = -1$, respectively. If the "dark state" is detected, the state is projected to the manifold $\{|1\rangle,|2\rangle\}$, and the motional state will not be affected. Otherwise, the state is projected to $|0\rangle$ and the motional state will be heated up to the Doppler cooling limit. Therefore, $150\mu s$ EIT cooling followed by $10\mu s$ optical pumping pulses are applied to bring it back to $|0\rangle$ and motional ground state, without affecting the "dark state".

of two sequence measurement boxes M_i and M_j associated with the observables A_i and A_j, respectively. Each measurement box M_i is implemented by a unitary rotation U_i, followed by a measurement in the standard basis which detects projection to the state $|0\rangle$ and an inverse unitary rotation $U_i^\dagger$. The rotation U_i as well as the corresponding measurement box M_i are uniquely determined by the observable A_i and are implemented in the same way in the experiments when we measure the correlation of A_i with other compatible observables to assure context independence. The measurement of observables are chosen randomly in our experiment using a quantum random number generator (QRNG).

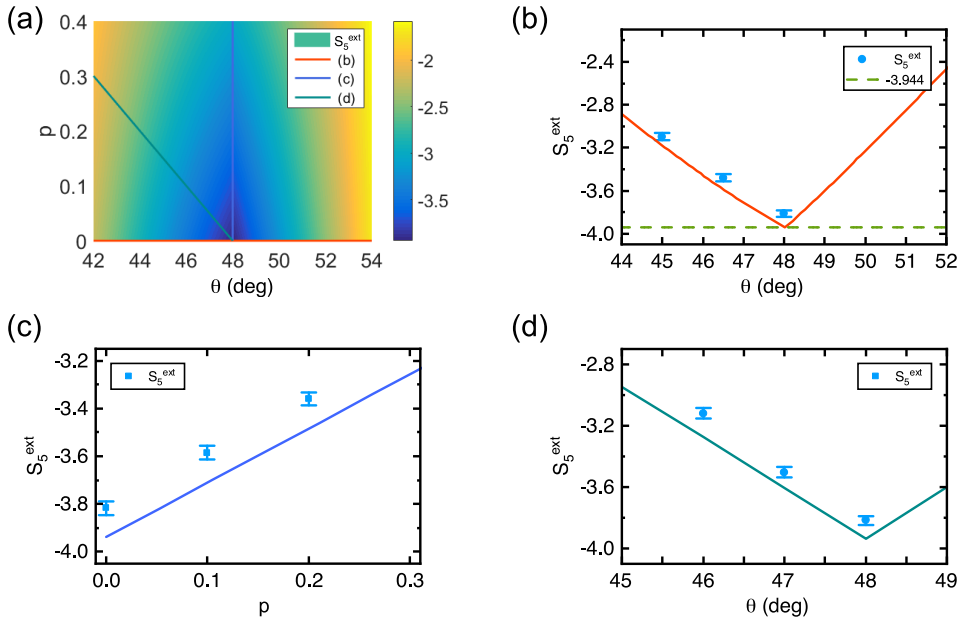

Figure 2. Experimental results, (a) The theoretical value of KCBS changes with θ and p. In the experiment, we observe the violation of KCBS in three tangent plane. (b) represents that the value of S_5^{ext} inequality increases with the change of measurement angle θ. For experiment point, $\theta == 48^o, 46.5^o, 45^o$ (c) represents that the S_5^{ext} inequality increases with the increase of p. For experiment point, $p == 0, 0.1, 0.2$. (d) represents that the S_5^{ext} inequality increases with the change of θ and p simultaneously. For experiment point, $\{\theta, p\} = \{48^o, 0\}, \{47^o, 0.05\}, \{46^o, 0.1\}$. The blue dot represents the experimental value, and the solid line represents the theoretical line.

Every data point measured for an observable A_i consists of the measurement ray v_i and an outcome $a = \pm 1$. From the full data set, we collect the numbers $N(A_i = a_1)$ and $N(A_i = a_1, A_j = a_2)$, where A_i and A_j are successful measurements in that order, $a_1, a_2 \in \{\pm 1\}$. Based on these numbers, we compute the expectation values,

$$\begin{aligned} \langle A_i \rangle &= \frac{\sum_{a_1} a_1 N\left(A_i = a_1\right)}{\sum_{a_1} N\left(A_i = a_1\right)} \\ \langle A_i A_j \rangle &= \frac{\sum_{a_1,a_2} a_1 a_2 N\left(A_i = a_1, A_j = a_2\right)}{\sum_{a_1,a_2} N\left(A_i = a_1, A_j = a_2\right)} \end{aligned} \tag{3}$$

In our experiment, we measure KCBS_5 inequalities. In order to avoid compatibility loophole, we choose "extended qualities" to address this problem[9, 10].

$$S_n^{(\mathrm{ext}\pm)} = \sum_{i=1}^{n} \left\langle A_i^{(1)} A_{i\pm1}^{(2)} \right\rangle + \sum_{i=1}^{n} \epsilon_i \geq S_n^{\mathrm{NC}} \tag{4}$$

where $\epsilon_i = \left| \left\langle A_i^{(1)} \right\rangle - \left\langle A_i^{(2)} \right\rangle \right|$. In order to reduce the statistical error of the data, 10,000 measurements were made on each measurement base.

Nonideal State and Measurement.— In order to demonstrate the performance of robustness of contextuality self-testing in the case of imperfect state preparation of $|v_0\rangle$ and measurement of $|v_1\rangle - |v_5\rangle$. We prepare the imperfect states and measurements. As shown in Fig. 2 (a), the violation of KCBS inequality can be changed by changing the angle "θ" for measurement and state $|v_0\rangle$.

First we change the measurement. We would introduce the first set of experiments in which a group of $n = 5$ states $|v_i\rangle$ on a "qutrit sphere" of superpositions of the basis state $|0\rangle$, $|1\rangle$, and $|2\rangle$ are measured. The pentagon states are given by

$$|v_i\rangle = U_i^\dagger |0\rangle\,, \text{ where } U_i^\dagger = R_z^{i-1}(\frac{4\pi}{5}) R_y(\theta), \tag{5}$$

where $R_y(\theta)$ indicates rotating around $|2\rangle$ (associated with y axis) and $R_z^{i-1}(\frac{4\pi}{5})$ indicates rotating around $|0\rangle$ (associated with z axis). As shown in Fig. 2 (b), we select $\theta = 48^o$, 46.5^o and 45^o, and we observe that the violation of inequality is significantly reduced.

After that, we mix some maximum mixed states into the state preparation:

$$\rho_0 = (1-p)|v_0\rangle\langle v_0| + \frac{p}{9} I. \tag{6}$$

As shown in Fig. 2 (c), we select $p = 0$, 0.1 and 0.2, and we observe that the violation of inequality is significantly reduced.

Finally, we change the θ and the state $|v_0\rangle$ simultaneously. As shown in the Fig. 2 (d), we choose $\{\theta, P\}=$

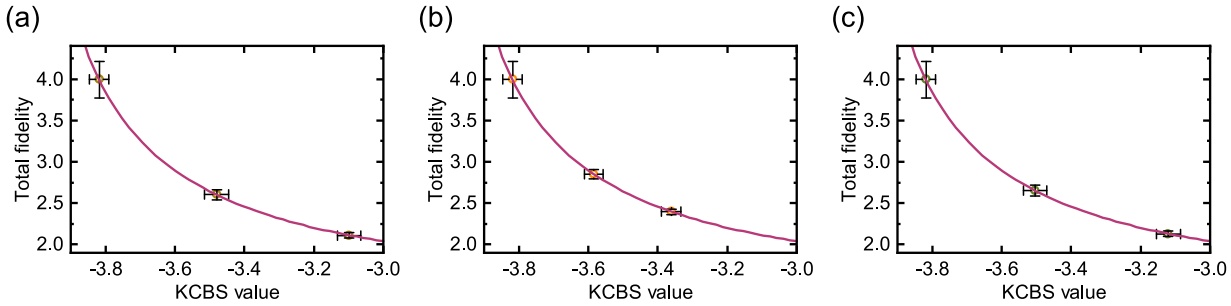

Figure 3. Self-testing fidelity. The solid line represents the minimum total fidelity variation with KCBS inequality violation. (a) is the fidelity obtained by self-testing after changing the measurement angle θ(p=0,$\theta = 48^o, 46.5^o, 45^o$). (b) is the fidelity obtained by self-testing after changing the white noise p(θ = 48,p=0,0.1,0.2).(c) is the fidelity obtained by self-testing after changing the θ and p simultaneously $(\theta, p = \{48^o, 0\}, \{47^o, 0.05\}, \{46^o, 0.1\})$.

$\{48^o, 0\}$, $\{47^o, 0.05\}$,$\{46^o, 0.1\}$. The violation value of KCBS inequality has changed significantly. All the details are shown in supplementary materials.

All the results are shown in Fig. 3.

Table I. Total fidenlity

θ, p	48°, 0	46.5°, 0	45°, 0
$KCBS_5$	-3.818(0.028)	-3.480(0.034)	-3.098(0.034)
Total Fidenlity	3.993(0.223)	2.600(0.058)	2.111(0.029)
θ, p	48°, 0	48°, 0.1	48°, 0.2
$KCBS_5$	-3.818(0.028)	-3.585(0.027)	-3.361(0.028)
Total Fidenlity	3.993(0.223)	2.851(0.059)	2.396(0.031)
θ, p	48°, 0	47°, 0.05	46°, 0.1
$KCBS_5$	-3.818(0.028)	-3.504(0.034)	-3.12(0.034)
Total Fidenlity	3.993(0.223)	2.651(0.067)	2.129(0.032)

Conclusions.— In this work, we provided the robustness curve corresponding to the local self-testing protocol based on KCBS inequality by using semidefinite programming with moment matrices. The aforementioned curve renders the results of [6] amenable to experimental scenarios. Using a single trapped $^{40}Ca^+$ ion, we provided an experimental demonstration of the self-testing protocol in [6].

In future, it would be interesting to improve the robustness curve. Memory loophole, more complicated scenario self-testing, IID, parallel repetition, self-testing high dimensional systems based on anticycle self-testing, analytically calculating the robustness constant based on techniques from convex optimization

[1] D. Mayers and A. Yao, Quantum Info. Comput. **4**, 273 (2004).
[2] I. Šupić and J. Bowles, Quantum **4**, 337 (2020).
[3] W.-H. Zhang, G. Chen, X.-X. Peng, X.-J. Ye, P. Yin, Y. Xiao, Z.-B. Hou, Z.-D. Cheng, Y.-C. Wu, J.-S. Xu, *et al.*, Physical Review Letters **121**, 240402 (2018).
[4] W.-H. Zhang, G. Chen, X.-X. Peng, X.-J. Ye, P. Yin, X.-Y. Xu, J.-S. Xu, C.-F. Li, and G.-C. Guo, Physical Review Letters **122**, 090402 (2019).
[5] Y. Liu, X. Yuan, M.-H. Li, W. Zhang, Q. Zhao, J. Zhong, Y. Cao, Y.-H. Li, L.-K. Chen, H. Li, *et al.*, Physical review letters **120**, 010503 (2018).
[6] K. Bharti, M. Ray, A. Varvitsiotis, N. A. Warsi, A. Cabello, and L.-C. Kwek, Phys. Rev. Lett. **122**, 250403 (2019).
[7] K. Bharti, M. Ray, A. Varvitsiotis, A. Cabello, and L.-C. Kwek, arXiv preprint arXiv:1911.09448 (2019).
[8] T. Metger and T. Vidick, arXiv preprint arXiv:2001.09161 (2020).
[9] J. V. Kujala, E. N. Dzhafarov, and J.-Å. Larsson, Physical Review Letters **115**, 150401 (2015).
[10] M. Malinowski, C. Zhang, F. M. Leupold, A. Cabello,

J. Alonso, and J. P. Home, Physical Review A **98**, 050102 (2018).
[11] A. Cabello, S. Severini, and A. Winter, Phys. Rev. Lett. **112**, 040401 (2014).
[12] F. M. Leupold, M. Malinowski, C. Zhang, V. Negnevitsky, A. Cabello, J. Alonso, and J. P. Home, Physical review letters **120**, 180401 (2018).
[13] Y. Pan, J. Zhang, E. Cohen, C.-w. Wu, P.-X. Chen, and N. Davidson, arXiv preprint arXiv:1910.11684 (2019).
[14] J. Zhang, F.-g. Li, Y. Xie, C.-w. Wu, B.-q. Ou, W. Wu, and P.-x. Chen, Physical Review A **98**, 052323 (2018).
[15] G. Chiribella and X. Yuan, arXiv preprint arXiv:1404.3348 (2014).
[16] R. Thew, K. Nemoto, A. G. White, and W. J. Munro, Physical Review A **66**, 012303 (2002).
[17] J. Fiurášek, Physical Review A **64**, 024102 (2001).

Appendix A: Robust self-testing via non-contextuality inequalities

Graph approach to contextuality— An arbitrary experimental scenario can be characterized by a set of measurement events $e_1, \ldots, e_n$. Two events are mutually exclusive if they correspond to same measurement but different outcomes. The exclusivity structure of a set of measurement events is captured by the exclusivity graph, denoted $\mathcal{G}_{\text{ex}}$, with nodes $\{1, \ldots, n\}$ (denoted by $[n]$) corresponding to events $\{e_i\}_{i=1}^n$. Two nodes i and j are adjacent (denoted by $i \sim j$) if e_i and e_j are mutually exclusive.

Given an experimental scenario with exclusivity graph $\mathcal{G}_{\text{ex}}$, a theory assigns probability to the events corresponding to its vertices. The mapping $p : [n] \to [0, 1]$, where $p_i + p_j \leq 1$, for all $i \sim j$ is called a behaviour. Here, the non-negative numbers p_i refer to the probability of the event e_i. We call a behaviour p deterministic non-contextual if all the probabilities p_i are either 0 or 1 and the occurrence of a event does not depend on the possibility of occurrence of other events. The convex hull of all deterministic non-contextual behaviours form a polytope, denoted by $\mathcal{P}_{nc}(\mathcal{G}_{\text{ex}})$, which contains all possible non-contextual behaviours for the experimental scenario encoded by the graph $\mathcal{G}_{\text{ex}}$. The behaviours which lie outside $\mathcal{P}_{nc}(\mathcal{G}_{\text{ex}})$ are contextual behaviours. The set of non-contextual behaviours are bounded by finitely many halfspaces, which are called non-contextuality inequalities. Formally speaking, non-contextuality inequalities correspond to linear inequalities of the form

$$\sum_{i\in[n]} w_i p_i \leq B_{nc}(\mathcal{G}_{\text{ex}}, w), \ \forall p \in \mathcal{P}_{nc}(\mathcal{G}_{\text{ex}}), \tag{A1}$$

where $w_1, \ldots, w_n \geq 0$ and $B_{nc}(\mathcal{G}_{\text{ex}}, w)$ are real scalars. The non-contextuality inequalities with all the weights $\{w_i\text{s}\}$ equal to one will be referred to as canonical non-contextuality inequalities. By definition, $B_{nc}(\mathcal{G}_{\text{ex}}, w)$ corresponds to the NCHV bound on the linear expression $\sum_{i\in[n]} w_i p_i$ and is also equal to the independence number of the exclusivity graph $\mathcal{G}_{\text{ex}}$, defined as the cardinality of the largest set of pairwise non-adjacent nodes of $\mathcal{G}_{\text{ex}}$ [11]. A quantum behaviour has the following form:

$$p_i = \text{tr}(\rho\Pi_i), \forall i \in [n] \text{ and } \text{tr}(\Pi_i\Pi_j) = 0, \text{ for } i \sim j, \tag{A2}$$

for some quantum state ρ and quantum projectors $\Pi_1, \ldots, \Pi_n$ acting on a Hilbert space $\mathcal{H}$. An ensemble $\rho, \{\Pi\}_{i=1}^n$ satisfying (A2) is called a *quantum realisation* of the behavior p. For a given quantum behaviour p, there can be multiple quantum realisations. The set of quantum behaviours is a convex set, which we denote by $\mathcal{P}_q(\mathcal{G}_{\text{ex}})$. The maximum value of the linear expression $\sum_{i\in[n]} w_i p_i$, as p ranges over the set of quantum behaviors $\mathcal{P}_q(\mathcal{G}_{\text{ex}})$ can exceed the classical bound. We will denote the maximum attainable quantum value by $B_{cq}(\mathcal{G}_{\text{ex}}, w)$. Interestingly, $B_{cq}(\mathcal{G}_{\text{ex}}, w)$ is equal to the *Lovász theta number* of the graph $\mathcal{G}_{\text{ex}}$ and admits a formulation as a tractable optimisation problem known as a semidefinite program [11].

Robust self-testing— Informally speaking, a non-contextuality inequality $\mathcal{I}$ is said to self-test a quantum realisation $\rho, \{\Pi\}_{i=1}^n$ if it achieves the quantum bound for the non-contextuality inequality $\mathcal{I}$ and furthermore, all other quantum realisations which achieve the quantum bound corresponding to $\mathcal{I}$ are equivalent to $\rho, \{\Pi\}_{i=1}^n$ up to global isometry. For a formal definition, the reader is referred to Section **??** in the Appendix. As discussed in [6], the essential ingredient in proving self-testing results for a non-contextuality inequality $\mathcal{I}$ with underlying exclusivity graph $\mathcal{G}_{\text{ex}}$ is that the corresponding Lovász theta semidefinite program (cf. (P_G)) has an unique optimal solution. In the case of the KCBS inequality, the exclusivity graph is a pentagon. The configuration corresponding to optimal quantum violation admits an umbrella structure. The KCBS inequality has been generalized to odd n-cycle exclusivity graphs, which are called KCBS_n inequalities. The KCBS_n inequalities are the canonical non-concontextuality inequalities for an odd cycle graph and admit robust self-testing [6].

A semidefinite program (SDP) is given by an optimisation problem of the following form

$$\sup_X \left\{ \langle C, X\rangle : X \in \mathcal{S}_+^n, \ \langle A_i, X\rangle = b_i \ (i \in [m]) \right\}, \tag{P}$$

where $\mathcal{S}_+^n$ denotes the cone of $n \times n$ real positive semidefinite matrices and $\langle X, Y\rangle = \text{tr}(X^T Y)$. The corresponding dual problem is given by

$$\inf_{y,Z} \left\{ \sum_{i=1}^m b_i y_i \ : \ \sum_{i=1}^m y_i A_i - C = Z \in \mathcal{S}_+^n \right\}. \tag{D}$$

A pair of primal-dual optimal solutions (X^*, Z^*) with no duality gap (i.e. $\text{tr}(X^* Z^*) = 0$), satisfies *strict complementarity* if

$$\text{rank}(X^*) + \text{rank}(Z^*) = n. \tag{A3}$$

Lastly, an optimal dual solution Z^* is called *dual non-degenerate* if the linear system in the symmetric matrix variable M

$$MZ^* = \mathrm{Tr}(MA_1) = \ldots = \mathrm{Tr}(MA_m) = 0,$$

only admits the trivial solution $M = 0$.

Central to this work is the Lovász theta SDP corresponding to a graph G, whose primal formulation is:

$$\begin{aligned} \vartheta(G) = \max \ & \sum_{i=1}^{n} X_{ii} \\ \text{s.t. } & X_{ii} = X_{0i}, \ i \in [n], \\ & X_{ij} = 0, \ i \sim j, \\ & X_{00} = 1, \ X \in \mathcal{S}_+^{1+n}, \end{aligned} \tag{P_G}$$

and the dual formulation we use is given by:

$$\begin{aligned} \vartheta(G) = \min \ & Z_{00} \\ \text{s.t. } & Z_{ii} = -(2Z_{0i} + 1), \ i \in [n], \\ & Z_{ij} = 0, \ i \nsim j, \\ & Z \in \mathcal{S}_+^{1+n}. \end{aligned} \tag{D_G}$$

A non-contextuality inequality $\sum_{i\in[n]} w_i p_i \leq B_{nc}(\mathcal{G}_{\mathrm{ex}}, w)$ is a *self-test* for the realisation $\{|u_i\rangle\langle u_i|\}_{i=0}^n$ if:

1. $\{|u_i\rangle\langle u_i|\}_{i=0}^n$ achieves the quantum supremum $B_{qc}(\mathcal{G}_{\mathrm{ex}}, w)$;
2. For any other realisation $\{|u_i'\rangle\langle u_i'|\}_{i=0}^n$ that also achieves $B_{qc}(\mathcal{G}_{\mathrm{ex}}, w)$, there exists an isometry V such that

$$V|u_i\rangle\langle u_i|V^\dagger = |u_i'\rangle\langle u_i'|, \quad 0 \leq i \leq n. \tag{A4}$$

Furthermore, a non-contextuality inequality $\sum_{i\in[n]} w_i p_i \leq B_{nc}(\mathcal{G}_{\mathrm{ex}}, w)$ is an (ϵ, r)-*robust self-test* for $\{|u_i\rangle\langle u_i|\}_{i=0}^n$ if it is a self-test, and furthermore, for any other realisation $\{|u_i'\rangle\langle u_i'|\}_{i=0}^n$ satisfying

$$\sum_{i=1}^{n} w_i |\langle u_i'|u_0'\rangle|^2 \geq B_{qc}(\mathcal{G}_{\mathrm{ex}}, w) - \epsilon,$$

there exists an isometry V such that

$$\| V|u_i\rangle\langle u_i|V^\dagger - |u_i'\rangle\langle u_i'| \| \leq \mathcal{O}\left(\epsilon^r\right), \quad 0 \leq i \leq n. \tag{A5}$$

Theorem 1. *Consider a non-contextuality inequality* $\sum_{i=1}^n w_i p_i \leq B_{nc}(\mathcal{G}_{\mathrm{ex}}, w)$. *Assume that*

1. *There exists an optimal quantum realisation* $\{|u_i\rangle\langle u_i|\}_{i=0}^n$ *such that*

$$\sum_i w_i |\langle u_i|u_0\rangle|^2 = B_{qc}(\mathcal{G}_{\mathrm{ex}}, w)$$

and $\langle u_0|u_i\rangle \neq 0$, *for all* $1 \leq i \leq n$, *and*

2. *There exists a dual optimal solution* Z^* *for the SDP* (D_G) *such that the homogeneous linear system*

$$\begin{aligned} M_{0i} &= M_{ii}, \ \textit{for all } 1 \leq i \leq n, \\ M_{ij} &= 0, \ \textit{for all } i \sim j, \\ MZ^* &= 0, \end{aligned} \tag{A6}$$

in the symmetric matrix variable M *only admits the trivial solution* $M = 0$.

Then, the non-contextuality inequality is an $(\epsilon, \frac{1}{2})$-*robust self-test for* $\{|u_i\rangle\langle u_i|\}_{i=0}^n$.

Experiment Setup.

We experimentally test these inequalities using a single trapped $^{40}Ca^+$ ion, which is confined in a blade-shaped Paul trap. The qutrit basis states are encoded into three Zeeman sub-levels of the $^{40}Ca^+$ ion, with $|1\rangle = \left|D_{5/2}, m_J = -3/2\right\rangle$, $|2\rangle = \left|D_{5/2}, m_J = -1/2\right\rangle$ and $|0\rangle = \left|S_{1/2}, m_J = -1/2\right\rangle$ [12].

Every experimental sequence starts with 1 ms Doppler cooling using a 397 nm laser, which is red detuned approximately half a natural linewidth from resonating with the cycling transition between $S_{1/2}$ and $P_{1/2}$ manifolds. This is followed by 300 μs EIT cooling and 1 ms sideband cooling, which cool the ion down to near the ground state. After that, 10 μs optical pumping laser is applied to initialize the qutrit to the $|0\rangle$ state with 99.8% fidelity. Subsequently, measurements of the observables $\{A_i\}$ are performed through coherent rotations between $|0\rangle$, $|1\rangle$ (at frequency ω_1) and $|0\rangle$, $|2\rangle$ (at frequency ω_2) with specific 729 nm laser beams. The rotation matrixes can be represented by $R_1(\theta_1, \phi_1)$ and $R_2(\theta_2, \phi_2)$ as shown in Fig.1. The angles $\theta_{1,2}$ and $\phi_{1,2}$ for a certain rotation are controlled by the duration and phase of the corresponding laser beam with high fidelity using acoustic-optic modulator. In our experiments the 2π time for both Rabi oscillation are adjusted to 142 μs, that is, the Rabi frequency is as low as $\Omega_{1,2} = (2\pi)7$ KHz, making the ac-Stark shift below 100 Hz. The separation between $|1\rangle$ and $|2\rangle$ is $\omega_2 - \omega_1 = (2\pi)8.69$ MHz with corresponding magnetic field $B = 5.18$ G. The maximum probability of off-resonant excitation $\Omega^2/(\omega_2 - \omega_1)^2$ is about 6.5×10^{-7}, small enough to ensure the independence of each Rabi oscillation [13, 14].

Fundamental Assumptions for Contextuality

For the contextuality self-testing experiment, we should try to reduce the dependence on the fundamental assumptions. For the ion trap experiment, there are compatibility, random selection of observables and sharp measurement hypothesis.

Detection efficiency A quantum jump detection is used to detect the probability in $\left|S_{1/2}\right\rangle$, which is the "bright state". The photons radiate from ion are collected through two objectives each with numerical aperture around NA = 0.32. In this experiment, we use two different settings of the detection laser for the first

and second photon detection steps. In the first detection step, the frequency of 397 nm laser is red detuned by half the nature linewidth and the laser intensity is set to lower level to minimize the heating effect, and the detection time is suppressed to 220 μs to minimize the random phase accumulation and decoherence. We observe on average 12 photons for the state $|0\rangle$ and less than 2.5 photons for the state $|1\rangle$ or $|2\rangle$. That is to say, the threshold value to distinguish bright state and dark state is set to $n_{ph} = 2.5$. The state detection error rates for wrongly registering the state $|0\rangle$ and missing the state $|0\rangle$ are 0.07% and 0.2%, respectively. For the second detection step, the laser frequency is set to on resonance. Together with 6 times higher laser power and 300 μs detection time, detection error is further suppressed. We observe on average 41 photons for the state $|0\rangle$ and 0.3 photons for the state $|1\rangle$ or $|2\rangle$. By setting the threshold to $n_{ph} = 8.5$, the state detection error rates for wrongly registering the state $|0\rangle$ and missing the state $|0\rangle$ are far less than 0.04%. Because the detection efficiency of ion trap is close to 100%, there is no detection efficiency loophole.

Compatibility Generally, two observables are compatible if measurements on them yield the same result regardless of whether they are performed simultaneously or sequentially in any temporal order, and regardless of the number of times they are measured. However, the perfect compatibility is never impossible to achieve in real experiments. One approach to address this problem is "extended inequalities"[9, 10]:

$$S_n^{(\mathrm{ext}\pm)} = \sum_{i=1}^{n} \left\langle A_i^{(1)} A_{i\pm1}^{(2)} \right\rangle + \sum_{i=1}^{n} \epsilon_i \geq \ S_n^{\mathrm{NC}} = -(n-2), \tag{A7}$$

where $\epsilon_i = \left| \left\langle A_i^{(1)} \right\rangle - \left\langle A_i^{(2)} \right\rangle \right|$. Note that this inequality is valid for both normal and inverse order measurements (indicated by $S_n^{(\mathrm{ext})+}(\theta)$ and $S_n^{(\mathrm{ext})-}(\theta)$ respectively). The extended term ϵ_i should, ideally be 0 if the two observables $A_i^{(1)}$ and $A_{i\pm1}^{(2)}$ are completely compatible. Because the result of measurement A_i should be the same weather it is performed before or after another measurement. Nevertheless, in a realistic experiment the result of two measurement on the same observable are hard to be identical. The experimental results for the S_5^{ext} , together with theoretical expectations for an ideal experiment are shown in Table I-Table VIII.

In order to confirm the non-disturbance of compatible measurements condition, we test whether the following four probabilities are equal: $p(M_i = 1|(M_i, M_{i+1}))$, $p(M_i = 1|(M_i, M_{i-1}))$,$p(M_i = 1|(M_{i+1}, M_i))$,$p(M_i = 1|(M_{i-1}, M_i))$. See supplementary materials for details.

Random Selection of Observables The measurement of observables are chosen randomly in our experiment using a quantum random number generator (QRNG). Let's take the inequality of n = 5 as an example. As shown in Fig.1, before each measurement, we prepare the ions to the $|0\rangle$ state. First a random integer m between 1 and 10 is generated. The random number $i = \mathrm{Mod}(\mathrm{m}, 5)$ select a observable A_i from $A_1 - A_5$, with A_0 equal to A_5, Then, one of the two observables $A_{i\pm1}$ which are compatible with A_i is selected randomly by the sign of $5.5 - m$. The random integer from the RNG determining control sequences are updated in real time (pregenerated before every experiment). In this way, we avoid the observable free choice loophole.

Sharp measurements Sharp measurements are minimally disturbing [15] and repeatable measurements. That is to say, the outcome should ideally be the same if we perform repeated measurements under the same experimental conditions. An observable A_i consists of the projective measurement basis $|v_i\rangle$ and the outcome $a = \pm1$. Through collecting the number of $N(A_i = a, A_i = a)$ and the total number of experiments $N(A, A)$, sharp measurements could be quantified in a realistic experiment through the probability R [12]:

$$R = \frac{\sum_i N(A_i = a, A_i = a)}{N(A, A)} \tag{A8}$$

For two continuous measurement of observable A_i, the ideal probability would be 1 for all observables. In our experiment, all $R > 0.99$, the results are presented in Table X.

State and Measurement tomography.— In order to compare the effect of self-testing on quantum system. We have done state and measurement tomography for state and measurement. In this experiment, we prepare the initial state in $|0\rangle$ with 10 μs optical pumping. In order to find the fidelity of this initial state, we did state tomography according to the Ref. [16]. As for a qutrit, we can write the density matrix as $\rho = \frac{1}{3}\sum_{j=0}^{8} r_j \lambda_j$, where the λ_j are the SU(3) generators and identity operator λ_0. The measurement basis $\{|\psi_j\rangle\}$ used in state tomography are chosen to be $|0\rangle$, $|1\rangle$, $|2\rangle$, $(|0\rangle + |1\rangle)/\sqrt{2}$, $(|0\rangle + i|1\rangle)/\sqrt{2}$, $(|0\rangle + |2\rangle)/\sqrt{2}$, $(|0\rangle + i|2\rangle)/\sqrt{2}$, $(|1\rangle + |2\rangle)/\sqrt{2}$, $(|1\rangle + i|2\rangle)/\sqrt{2}$, and we make the projection operator $|\psi_j\rangle\langle\psi_j|$ as the generators. All the results are shown in Table IX.

We did measurement tomography according to Ref. [17]. The probability p_{lm} that the apparatus will respond with positive operator-values measure (POVM) Π_l when measuring the quantum state with density matrix can be expressed as $p_{lm} = \mathrm{Tr}[\Pi_l \rho_m]$, where Tr stands for the trace. Assuming that the theoretical detection probability p_{lm} can be replaced with relative experimental frequency f_{lm}, we may write $\mathrm{Tr}[\Pi_l \rho_m] = \sum_{i,j=1}^{N} \Pi_{l,ij} \rho_{m,ji} = f_{lm}$, where N is the dimension of Hilbert space on which the operators Π_l

act. Then we can reconstruct the POVM Π_l according to experimental result f_{lm}. The density matrix ρ_m chosen in this process are the same as projection operators $|\psi_j\rangle\langle\psi_j|$ in state tomography. Also the MLS method is used in this process to ensure $\Pi_l \geqslant 0$ and $\sum_{l=1}^{k} \Pi_l = I$, where k is the number of measurement outcomes. The result are shown in Table XI.

Appendix B: Technical Background; in progress

1. Exclusivity graph approach to contextuality

2. Robust self-testing

- Definition
- Statement for KCBS [PRL]
- Robustness curve is missing! Or is it?

Appendix C: Robustness Curve

[DISCLAIMER: I am writing the following as rough notes which may ramble but should at least be consistent; in the following iteration, I hope to make improve the presentation]

What we have is some experimental data

1. Description

TODO:

- IID
- Restricted subspace or full subspace, Bell
- Parallel or Serial
  - When IID, parallel and serial should become identical
  - When not IID, parallel should be more general
- Clarify the issue with the sum

Consider the KCBS scenario, i.e. an experimental scenario which is specified by the events $e_1, e_2 \dots e_5$ whose exclusivity is given by a 5-cycle exclusivity graph. Suppose we obtain the probabilities $p_1, p_2 \dots p_5$ experimentally (and ensure that they correspond to sharp measurements). We already saw that if these values nearly saturate the quantum bound for the KCBS non-contextuality inequality, i.e. $\sum_{i=1}^{5} p_i$ approaches $\sqrt{5} \approx 2.236\dots$, then we know that all quantum realisations corresponding to the experimentally obtained probabilities $\{p_i\}_{i=1}^5$ are almost equivalent to $\rho^{\text{KCBS}}, \{\Pi_i^{\text{KCBS}}\}_{i=1}^5$, up to a global isometry. To be more precise, consider any arbitrary quantum realisation given by a pure state ρ and rank one projectors $\{\Pi_i\}$ such that $\sum_{i=1}^{5} p_i = 2 + \epsilon$. It was shown in [**?**] that then, there exists an isometry V such that

$$\left\| V\Pi_i V^\dagger - \Pi_i^{\text{KCBS}} \right\|_F \leq \mathcal{O}(\sqrt{\epsilon}) \tag{C1}$$

for all $i \in \{1, 2 \dots 5\}$ and $\left\| \rho - \rho^{\text{KCBS}} \right\|_F \leq \mathcal{O}(\sqrt{\epsilon})$ where $\|A\|_F := \text{tr}\left(\sqrt{A^\dagger A}\right)$. [Verify this:] This result is stronger than the self-testing results which are usually stated for Bell non-locality, in the following sense. Typically, one is only able to make statements about the action of the projectors Π_i on the state ρ (see, for instance, ...). Despite this, without the constant hidden in **??**, one cannot obtain a robustness curve and thus one cannot apply this in practice. In this work, we remedy this problem, taking inspiration from the Bell self-testing approach. To this end, we give a slightly different statement: we show that

$$\sum_{i=1}^{5} \mathcal{F}(V\Pi_i\rho\Pi_i V^\dagger, \Pi_i^{\text{KCBS}}\rho^{\text{KCBS}}\Pi_i^{\text{KCBS}}) + \mathcal{F}(V\rho V^\dagger, \rho^{\text{KCBS}}) \geq f(\epsilon) \tag{C2}$$

where $\mathcal{F}(A, B) := \text{tr}\sqrt{\left|A^{1/2}B^{1/2}\right|}$, we only require Π_i to be projectors and allow ρ to be a mixed state. The advantage is that we are able to express $f(\epsilon)$ as a hierarchy of semi-definite programmes and compute lower bounds explicitly. While we state our result for the KCBS inequality, it readily extends to the n-cycle scenario. [TODO: if f cannot be shown to be independent of the individual p_is, then we must skip it].

2. Overall Strategy

TODO

- Verify if we require that $\Pi_i\Pi_j = 0$ or that $\text{tr}[\Pi_i\Pi_j\rho] = 0$. $\text{tr}[\Pi_i\Pi_j\Pi_k\rho]$ (by assumption; write clearly in the previous section)

We may restate the aforesaid discussion more symbolically as lower bounding the value of the following objective function:

$$F := \min_{\rho, \{\Pi_i\}} \max_{V} \left[\sum_{i=1}^{5} \mathcal{F}(V\Pi_i\rho\Pi_i V^\dagger, \Pi_i^{\text{KCBS}}\rho^{\text{KCBS}}\Pi_i^{\text{KCBS}}) + \mathcal{F}(V\rho V^\dagger \right.$$

where $\rho, \{\Pi_i\}_{i=1}^5$ is a quantum realisation[1] of $\{p_i\}_{i=1}^5$, V is an isometry from $\mathcal{H}$ to $\mathcal{H}^{\text{KCBS}}$, i.e. from the space on which $\rho, \{\Pi_i\}_{i=1}^5$ act/are defined to that where $\rho^{\text{KCBS}}, \{\Pi_i^{\text{KCBS}}\}_{i=1}^5$ act/are defined. At the broadest level, the idea is to drop the maximization over V with

[1] note that we assume Π_i are projectors as the measurements are assumed to be sharp experimentally

a particular isometry V which is expressed in terms of $\rho, \{\Pi_i\}_{i=1}^5$. Then, as we shall see, the expression for the fidelity appears as a sum of terms of the following form. Let w be a word created from the letters, $\{\mathbb{I}, \Pi_1, \Pi_2 \ldots \Pi_5, \hat{P}\}$ with $\hat{P}^\dagger \hat{P} = \mathbb{I}$, $\Pi_i^2 = \Pi_i$ and $\Pi_i \Pi_j = 0$ if $(i,j) \in E(G)$, i.e. when i, j are exclusive[2]. The fidelity is a linear combination of these words, i.e. $F = \min_{\{\langle w \rangle\}} \sum_w \alpha_w \langle w \rangle$ where $\mathrm{tr}[w\rho] =: \langle w \rangle$, subject to the constraint that $\{\langle w \rangle\}_w$ corresponds to a quantum realisation. The advantage of casting the problem in this form is that one can now construct an NPA-like hierarchy. The idea is simple to state. Treat $\{\langle w \rangle\}_w$ as a vector. Denote by Q the set of all such vectors which correspond to a quantum realisation (of $\{p_i\}_{i=1}^5$). It turns out that one can impose constraints on words with k letters, for instance. Under these constraints, denote by Q_k the set that is obtained. Note that $Q_k \supseteq Q$ for it may contain vectors which don't correspond to the quantum realisation. In fact, Q_k can be characterised using semi-definite programming constraints (which in turn means they are efficiently computable). Intuitively, it is clear that $\lim_{k\to\infty} Q_k = Q$. Further, it is also clear that $F = \min_{\{\langle w \rangle\}_w \in Q} \sum_w \alpha_w \langle w \rangle \geq \min_{\{\langle w \rangle\}_w \in Q_k} \sum_w \alpha_w \langle w \rangle$ as we are minimising over a larger set on the right hand side.

We can now

- Regularizing the experimental statistics
- Constructing the isometry
- Deriving the expression for fidelity
- Providing the lower bound

The goal is to provide a lower bound on fidelity for the experimental results in section 2. The following steps are required:

3. Regularizing the experimental statistics [TODO: see later if this is still relevant]

In reference [**?**], authors assume that the measurement operators follow cyclic compatibility structure. However, this need not be true in the real life experimental scenario. Thus, the experimental data may not belong to quantum set due to finite statistics and violation of the cyclic compatibility structure. This demands a regularization of the experimental data for the theoretical analysis. Here, regularization means finding the statistics which is closest to our experimental statistics and belongs to the quantum set. The set of quantum behaviours forms a convex set, known as theta body.

4. Providing a lower bound on the fidelity from regularized measurement statistics

a. Constructing the isometry

A swap circuit between two qudit registers is given by $S = TUVU$ where

$$T = \mathbb{I} \otimes \sum_k |-k\rangle\langle k|$$

$$U = \sum_{k=0}^{d-1} P^k \otimes |k\rangle\langle k|$$

$$V = \sum_{k=0}^{d-1} |k\rangle\langle k| \otimes P^{-k}$$

and

$$P = \sum_{k=0}^{d-1} |k+1\rangle\langle k|.$$

Here, P is a translation operator.

TUVU, Localizing matrix etc....

b. Deriving the expression for fidelity

Let $\left\{\{\bar{\Pi}_i\}_{i\in V}, |\bar{\psi}\rangle\right\}$ be the ideal configuration and $\{\{\Pi_i\}, |\psi\rangle\}$ be the candidate configuration. Our expression for the fidelity for the aforementioned configurations is given by

$$F(\alpha, \beta) = \alpha \sum_{i\in V} \langle\bar{\psi}|\bar{\Pi}_i \Pi_i|\psi\rangle + \beta\langle\bar{\psi}|\psi\rangle,$$

where α,$\beta \in \mathbb{R}$ and are weights on fidelitiy for states and measured states respectively.

The total fidelity for state and projectors for odd n-cycle scenario in the ideal case is $n+1$.

c. Providing the lower bound on fidelity

NPA analoge for theta body

[2] We introduced $\hat{P}$ for completeness; its role is explained later.

48°	i	j	$\langle A_i \rangle$	$\langle A_j \rangle$	$\langle A_i A_j \rangle$
Ideal			0.105	0.105	-0.788
Ideal total			$S_5^{(\text{ext})} \approx -3.944$		
6*Normal	1	2	0.105(0.010)	0.104(0.010)	-0.770(0.006)
	2	3	0.101(0.010)	0.085(0.010)	-0.783(0.006)
	3	4	0.111(0.010)	0.110(0.010)	-0.761(0.006)
	4	5	0.086(0.010)	0.111(0.010)	-0.786(0.006)
	5	1	0.098(0.010)	0.104(0.010)	-0.785(0.006)
	total		$S_5 \approx -3.886(0.014), S_5^{(\text{ext})} \approx -3.818(0.028)$		

Table II. Experimental results for the KCBS experiment for the points angle $\theta = 48, p = 0$ in normal order.

48°	i	j	$\langle A_i \rangle$	$\langle A_j \rangle$	$\langle A_i A_j \rangle$
Ideal			0.105	0.105	-0.788
Ideal total			$S_5^{(\text{ext})} \approx -3.944$		
6*Reverse	1	5	0.101(0.010)	0.096(0.010)	-0.782(0.006)
	2	1	0.091(0.010)	0.114(0.010)	-0.764(0.006)
	3	2	0.109(0.010)	0.088(0.010)	-0.759(0.006)
	4	3	0.105(0.010)	0.094(0.010)	-0.769(0.007)
	5	4	0.084(0.010)	0.099(0.010)	-0.781(0.006)
	total		$S_5 \approx -3.854(0.015), S_5^{(\text{ext})} \approx -3.806(0.028)$		

Table III. Experimental results for the KCBS experiment for the points angle $\theta = 48, p = 0$ in reverse order.

46.5°	i	j	$\langle A_i \rangle$	$\langle A_j \rangle$	$\langle A_i A_j \rangle$
Ideal			0.052	0.139	-0.804
Ideal total			$S_5^{(\text{ext})} \approx -3.586$		
6*Normal	1	2	0.056(0.010)	0.149(0.010)	-0.762(0.007)
	2	3	0.054(0.010)	0.129(0.010)	-0.769(0.006)
	3	4	0.053(0.010)	0.137(0.010)	-0.778(0.006)
	4	5	0.050(0.010)	0.122(0.010)	-0.799(0.006)
	5	1	0.047(0.010)	0.139(0.010)	-0.789(0.006)
	total		$S_5 \approx -3.898(0.014), S_5^{(\text{ext})} \approx -3.480(0.034)$		

Table IV. Experimental results for the KCBS experiment for the points angle $\theta = 46.5^o, p = 0$ in normal order.

45°	i	j	$\langle A_i \rangle$	$\langle A_j \rangle$	$\langle A_i A_j \rangle$
Ideal			0	0.173	-0.809
Ideal total			$S_5^{(\text{ext})} \approx -3.181$		
6*Normal	1	2	-0.009(0.010)	0.188(0.010)	-0.783(0.006)
	2	3	0.014(0.010)	0.147(0.010)	-0.785(0.006)
	3	4	-0.002(0.010)	0.182(0.010)	-0.782(0.007)
	4	5	-0.009(0.010)	0.169(0.010)	-0.801(0.006)
	5	1	0.007(0.010)	0.155(0.010)	-0.787(0.006)
	total		$S_5 \approx -3.938(0.013), S_5^{(\text{ext})} \approx -3.098(0.034)$		

Table V. Experimental results for the KCBS experiment for the points angle $\theta = 45.0^o, p = 0$ in normal order.

$48^\circ, p = 0.1$	i	j	$\langle A_i \rangle$	$\langle A_j \rangle$	$\langle A_i A_j \rangle$
Ideal			0.128	0.128	-0.743
Ideal total			$S_5^{(\text{ext})} \approx -3.711$		
6*Normal	1	2	0.123(0.010)	0.126(0.010)	-0.722(0.007)
	2	3	0.118(0.010)	0.111(0.010)	-0.720(0.007)
	3	4	0.118(0.010)	0.129(0.010)	-0.715(0.007)
	4	5	0.103(0.010)	0.120(0.010)	-0.742(0.007)
	5	1	0.124(0.010)	0.116(0.010)	-0.739(0.007)
	total		$S_5 \approx -3.639(0.015), S_5^{(\text{ext})} \approx -3.585(0.027)$		

Table VI. Experimental results for the KCBS experiment for the points angle $\theta = 48^o, p = 0.1$ in normal order.

$48^\circ, p = 0.2$	i	j	$\langle A_i \rangle$	$\langle A_j \rangle$	$\langle A_i A_j \rangle$
Ideal			0.151	0.151	-0.698
Ideal total			$S_5^{(\text{ext})} \approx -3.489$		
6*Normal	1	2	0.150(0.010)	0.144(0.010)	-0.675(0.007)
	2	3	0.151(0.010)	0.135(0.010)	-0.672(0.007)
	3	4	0.139(0.010)	0.154(0.010)	-0.676(0.007)
	4	5	0.146(0.010)	0.145(0.010)	-0.681(0.008)
	5	1	0.135(0.010)	0.135(0.010)	-0.703(0.007)
	total		$S_5 \approx -3.407(0.017), S_5^{(\text{ext})} \approx -3.361(0.028)$		

Table VII. Experimental results for the KCBS experiment for the points angle $\theta = 48^o, p = 0.2$ in normal order.

$46^\circ, p = 0.1$	i	j	$\langle A_i \rangle$	$\langle A_j \rangle$	$\langle A_i A_j \rangle$
Ideal			0.065	0.169	-0.759
Ideal total			$S_5^{(\text{ext})} \approx -3.275$		
6*Normal	1	2	0.065(0.010)	0.161(0.010)	-0.724(0.007)
	2	3	0.062(0.010)	0.161(0.010)	-0.715(0.007)
	3	4	0.062(0.010)	0.182(0.010)	-0.721(0.007)
	4	5	0.054(0.010)	0.161(0.011)	-0.752(0.007)
	5	1	0.053(0.010)	0.167(0.010)	-0.745(0.007)
	total		$S_5 \approx -3.658(0.015), S_5^{(\text{ext})} \approx -3.120(0.034)$		

Table VIII. Experimental results for the KCBS experiment for the points angle $\theta = 46^o, p = 0.1$ in normal order.

$46^\circ, p = 0.05$	i	j	$\langle A_i \rangle$	$\langle A_j \rangle$	$\langle A_i A_j \rangle$
Ideal			0.083	0.138	-0.777
Ideal total			$S_5^{(\text{ext})} \approx -3.610$		
6*Normal	1	2	0.093(0.010)	0.128(0.010)	-0.751(0.007)
	2	3	0.071(0.010)	0.131(0.010)	-0.749(0.007)
	3	4	0.081(0.010)	0.138(0.010)	-0.742(0.007)
	4	5	0.082(0.010)	0.130(0.010)	-0.745(0.007)
	5	1	0.080(0.010)	0.125(0.010)	-0.762(0.006)
	total		$S_5 \approx -3.749(0.015), S_5^{(\text{ext})} \approx -3.504(0.034)$		

Table IX. Experimental results for the KCBS experiment for the points angle $\theta = 47^o, p = 0.05$ in normal order.

state	Fidelity to self	Fidelity to $\|0\rangle$
$\|0\rangle$	0.999(0.009)	0.999(0.007)
$\|1\rangle$	0.996(0.001)	0.004(0.001)
$\|2\rangle$	0.993(0.005)	0.006(0.001)
mixed with $p = 0.05$	0.999(0.003)	0.967(0.013)
mixed with $p = 0.1$	0.996(0.002)	0.935(0.015)
mixed with $p = 0.2$	0.992(0.003)	0.846(0.014)

Table X. Fidelity of the initial state.

sharp measurement	M_1	M_2	M_3	M_4	M_5	total
R	0.994(0.008)	0.991(0.008)	0.990(0.008)	0.9925(0.008)	0.9941(0.008)	0.9923(0.008)

Table XI. Sharp measurement, All results were obtained at $\theta = 48^o$.

θ	order	Fidelity	error
5*48°	1	0.994	0.006
	2	0.991	0.006
	3	0.996	0.008
	4	0.995	0.006
	5	0.990	0.010
5*47°	1	0.992	0.007
	2	0.986	0.005
	3	0.992	0.011
	4	0.989	0.006
	5	0.996	0.008
5*46.5°	1	0.989	0.006
	2	0.997	0.004
	3	0.998	0.007
	4	0.992	0.003
	5	0.988	0.010
5*46°	1	0.990	0.006
	2	0.990	0.005
	3	0.994	0.010
	4	0.995	0.006
	5	0.987	0.011
5*45°	1	0.988	0.006
	2	0.992	0.005
	3	0.988	0.011
	4	0.991	0.006
	5	0.983	0.010

Table XII. Fidelity of the POVM in different θ.

order	Probability	error
$p(M_1 = 1\|(M_1, M_2))$	0.553	0.005
$p(M_1 = 1\|(M_5, M_1))$	0.552	0.005
$p(M_1 = 1\|(M_2, M_1))$	0.557	0.005
$p(M_1 = 1\|(M_1, M_5))$	0.551	0.005
$p(M_2 = 1\|(M_1, M_2))$	0.552	0.005
$p(M_2 = 1\|(M_2, M_3))$	0.551	0.005
$p(M_2 = 1\|(M_2, M_1))$	0.546	0.005
$p(M_2 = 1\|(M_3, M_2))$	0.544	0.005
$p(M_3 = 1\|(M_2, M_3))$	0.543	0.005
$p(M_3 = 1\|(M_3, M_4))$	0.556	0.005
$p(M_3 = 1\|(M_3, M_2))$	0.555	0.005
$p(M_3 = 1\|(M_4, M_3))$	0.547	0.005
$p(M_4 = 1\|(M_3, M_4))$	0.555	0.005
$p(M_4 = 1\|(M_4, M_5))$	0.543	0.005
$p(M_4 = 1\|(M_4, M_3))$	0.553	0.005
$p(M_4 = 1\|(M_5, M_4))$	0.550	0.005
$p(M_5 = 1\|(M_4, M_5))$	0.556	0.005
$p(M_5 = 1\|(M_5, M_1))$	0.549	0.005
$p(M_5 = 1\|(M_5, M_4))$	0.542	0.005
$p(M_5 = 1\|(M_1, M_5))$	0.548	0.005

Table XIII. Non-disturbance of compatible measurements.